Focused RF hyperthermia using magnetic fluids

T. Onur Tasci
Department of Bioengineering, University of Utah, Salt Lake City, Utah 84112

Ibrahim Vargel
Department of Plastic and Reconstructive Surgery, Kirikkale University, 71100, Kirikkale, Turkey

Anil Arat
Department of Radiology, Baylor College of Medicine, Houston, Texas 77030

Elif Guzel
Department of Histology and Embryology, Cerrahpasa School of Medicine, 34098, Istanbul University, Istanbul, Turkey

Petek Korkusuz
Department of Histology and Embryology, Hacettepe University Faculty of Medicine, 06100, Sihhiye, Ankara, Turkey

Ergin Atalar[a)]
Department of Electrical and Electronic Engineering, Bilkent University, 06800, Ankara, Turkey

(Received 28 June 2008; revised 2 March 2009; accepted for publication 5 March 2009; published 27 April 2009)

Heat therapies such as hyperthermia and thermoablation are very promising approaches in the treatment of cancer. Compared with available hyperthermia modalities, magnetic fluid hyperthermia (MFH) yields better results in uniform heating of the deeply situated tumors. In this approach, fluid consisting of superparamagnetic particles (magnetic fluid) is delivered to the tumor. An alternating (ac) magnetic field is then used to heat the particles and the corresponding tumor, thereby ablating it. However, one of the most serious shortcomings of this technique is the unwanted heating of the healthy tissues. This results from the magnetic fluid diffusion from the tumor to the surrounding tissues or from incorrect localization of the fluids in the target tumor area. In this study, the authors demonstrated that by depositing appropriate static (dc) magnetic field gradients on the alternating (ac) magnetic fields, focused heating of the magnetic particles can be achieved. A focused hyperthermia system was implemented by using two types of coils: dc and ac coils. The ac coil generated the alternating magnetic field responsible for the heating of the magnetic particles; the dc coil was used to superimpose a static magnetic field gradient on the alternating magnetic field. In this way, focused heating of the particles was obtained in the regions where the static field was dominated by the alternating magnetic field. *In vitro* experiments showed that as the magnitude of the dc solenoid currents was increased from 0 to 1.8 A, the specific absorption rate (SAR) of the superparamagnetic particles 2 cm apart from the ac solenoid center decreased by a factor of 4.5, while the SAR of the particles at the center was unchanged. This demonstrates that the hyperthermia system is capable of precisely focusing the heat at the center. Additionally, with this approach, shifting of the heat focus can be achieved by applying different amounts of currents to individual dc solenoids. *In vivo* experiments were performed with adult rats, where magnetic fluids were injected percutaneously into the tails (with homogeneous fluid distribution inside the tails). Histological examination showed that, as we increased the dc solenoid current from 0.5 to 1.8 A, the total burned volume decreased from 1.6 to 0.2 cm^3 verifying the focusing capability of the system. The authors believe that the studies conducted in this work show that MFH can be a much more effective method with better heat localization and focusing abilities. © *2009 American Association of Physicists in Medicine*. [DOI: 10.1118/1.3106343]

Key words: hyperthermia, thermal ablation, magnetic fluids, magnetic fields, focused hyperthermia, tumor therapy

I. INTRODUCTION

Currently, various types of heat treatment modalities are available for the treatment of cancer such as microwave, ultrasound, focused ultrasound, radio frequency (RF) capacitance hyperthermia, RF probe hyperthermia, and magnetic fluid hyperthermia (MFH). Each treatment technique has certain limitations.[1–4] For instance, microwave hyperthermia has a poor depth of penetration, which makes it unsuitable for treatment of deep-seated tumors. Compared with microwave, ultrasound has better penetration depth and focusing abilities, but particular drawbacks of ultrasound include high energy absorption of the bone and liquid-containing organs and excessive reflection from the cavities filled with air. In

RF capacitance hyperthermia, the major limiting factor is the inability of the electric field to focus on the tumor, so that all the tissues that the electric field penetrated are heated. RF probe hyperthermia has the disadvantage of poor accessibility to the deep-seated tumors, with a limited accuracy of localization. Finally, this technique is not suitable for the treatment of large tumors.

Compared with the aforementioned methods, MFH is better in uniform heating of the deeply situated tumors with relatively good targeting.[1,4] Generally, in this technique, magnetic fluids are dispersed into the target tissue and, through the application of an external ac magnetic field, heating of the fluids is achieved.[5] Some of the limitations of magnetic fluid hyperthermia are the difficulty of temperature monitoring and quantification of the magnetic fluid distribution inside the tissue. However, the most important shortcoming of this technique is the unwanted heating of the healthy tissues resulting from the diffusion of fluids into the collateral tissues. Some methods to selectively tag the tumors with magnetic particles have been proposed,[6] but particle penetration to the surrounding healthy tissues still has not been significantly prevented. Since dispersion of the magnetic particles to normal tissues is currently unavoidable, a method to directly focus the heat on the tumors should be generated. In this study, we proposed and designed a system that focuses the heat into very small regions so that focused heating of magnetic particles, and therefore tumors, can be achieved by limiting the damage to the collateral healthy tissue. An analogous system has been demonstrated for the tomographic imaging of the magnetic particles by Gleich and Weizenecker.[7]

II. THEORY AND METHODS

It is well known that, under alternating magnetic fields, superparamagnetic (single domain) nanoparticles are heated as a result of the rotation of the particle itself (Brownian relaxation)[8] and the rotation of the magnetic moment inside the particle (Néel relaxation).[9] If a static magnetic field with equal or larger amplitude is superimposed on the alternating field, the single domain particles and their magnetic moments will align with the static field. In this way, Néel and Brownian relaxations will be blocked and the heating of the particles will be diminished. This effect has been shown in previous studies[5,10] in which a static magnetic field, perpendicular to the ac field, was applied to magnetic fluids (colloidal dispersions of superparamagnetic iron oxide particles) and it was observed that heating was significantly reduced when the amplitude of the static field approached that of the alternating field. These studies demonstrate that static magnetic fields can be used to modulate the heating effect of ac magnetic fields on the magnetic domains.

In traditional MFH systems, magnetic particles that have been dispersed into the tissue are heated by application of ac magnetic fields. In this process, unselective heating of the particles occurs because all the particles exposed to the alternating field are heated equally. By depositing appropriate dc magnetic field gradients on the ac magnetic fields, one can generate ac field dominant regions and achieve focused heating of the magnetic particles in these regions. Figure 1 shows a system that accomplishes this task. In this system, the two solenoids on the right and left of the figure are excited with equal but opposite dc currents. The static field vectors generated by the solenoids cancel each other at the center of the system and a region with a very small dc magnetic field is formed around the center, which can be named as the field-free region (FFR). If an alternating magnetic field is applied to the space between the solenoids, the alternating field will be dominant in the FFR and only the magnetic particles inside the FFR will be heated. The particles outside this region cannot be heated as a result of the dominance of the static field on the alternating field. The field-free region explained above can be reduced further (i.e., more intense heat focus can be obtained) by increasing the current magnitudes flowing through the dc solenoids. In addition, the position of the focus can be changed by giving different amplitudes of currents to the individual dc solenoids.

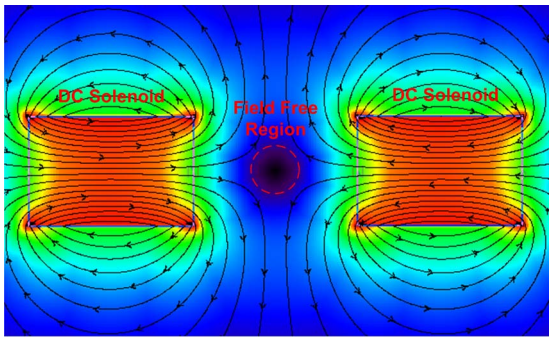

FIG. 1. Opposed dc solenoids produce a FFR in the middle of the solenoids. If an additional ac magnetic field is applied between the solenoids only the particles in the FFR will be heated and focused heating of the particles will be achieved. (This figure is created by VIZIMAG 3.14 software.)

Figure 2(a) is a schematic of the focused heating applicator architecture used in our experiments. This setup builds on Fig. 1 by the addition of an ac solenoid between the two dc solenoids. This ac solenoid generates the alternating magnetic field that is responsible for the heating of the magnetic particles. Other lateral solenoids (dc solenoids) generate a static magnetic field gradient such that a field-free region is generated in their middle.

To test the explained focused heating system, several *in vitro* and *in vivo* experiments were conducted using the experimental setup shown in Fig. 2. Air-cored copper solenoids of equal size (coil length is equal to 6 cm, inner and outer coil radii are 2 and 2.9 cm, respectively) were obtained from DAYM (Ders Aletleri Yapim Merkezi, Ankara, Turkey). 1200 turn coils (35 mH) were used as the dc solenoids and a 300 turn coil (2.7 mH) was used as the ac solenoid. The sinusoidal voltage was applied via the signal generator (Stanford Research Systems, Sunnyvale, CA, DS345) and was passed to the amplifier input, whose output connected to the matching circuit of the ac solenoid. The dc power supply (HP E3616 A) was connected directly to the dc solenoids to produce the necessary static magnetic field gradient. For the

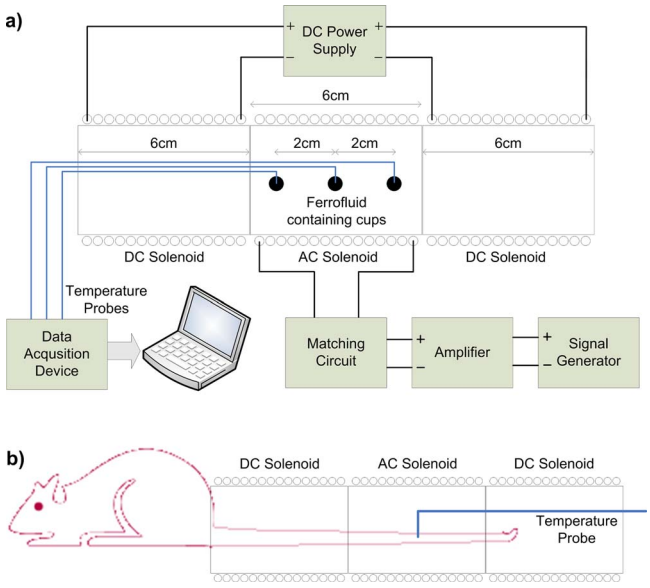

FIG. 2. (a) General experimental setup used in the experiments. (b) *In vivo* experiment setup.

continuous temperature measurements, fiber optic temperature probes (FISO Technologies, Ste. Foy, Quebec, Canada) were inserted into the point of interest.

During the standard operation of the system the ac coil would heat up due to skin and proximity effects.[11,12] Additionally the very high static current of the dc solenoids would cause considerable heating in the copper coils. To overcome this excessive heating in the coils, water was circulated through the interior of the solenoids for cooling.

III. EXPERIMENTS

To validate the focused heating ability of the hyperthermia system, several *in vitro* and *in vivo* experiments were made.

III.A. *In vitro* experiments

A schematic of the *in vitro* experiment is shown in Fig. 2(a). Three spherical plastic cups of diameter of 0.4 cm were placed inside the ac solenoid. The cups were filled with a magnetic fluid with an average core size of 10 nm in which the weight fraction of magnetite was slightly larger than 20% (Liquids Research Ltd., Bangor, Gwynedd, Wales, www.liquidsresearch.co.uk). The first cup was placed at the center (inside the FFR) and other two were placed 2 cm to the left and right of the central cup. An ac magnetic field, with strength of 4.5 kA/m at 80 kHz, was applied and the resulting temperature increase in each of the cups was recorded for varying dc magnetic field conditions, corresponding to dc solenoid currents (IDC) of 0, 0.5, 1, and 1.8 A. Simultaneous temperature measurements were made using the fiber optic temperature probes. Obtained temperature versus time graphs can be seen in Fig. 3. From these graphs, by using the rate of temperature rise method ($c*\Delta T/\Delta t$), specific absorption rate (SAR) calculations were made and tabulated as shown in Table II of Sec. IV. Here, c is the specific heat of the heated magnetic material and ΔT is the differential increase in the temperature for a differential time of Δt s.

Another *in vitro* experiment was performed using the same setup. In this case, different current magnitudes of 0.2 and 1.8 A were applied to the left and right solenoids. The aim of applying different magnitudes of currents is to show

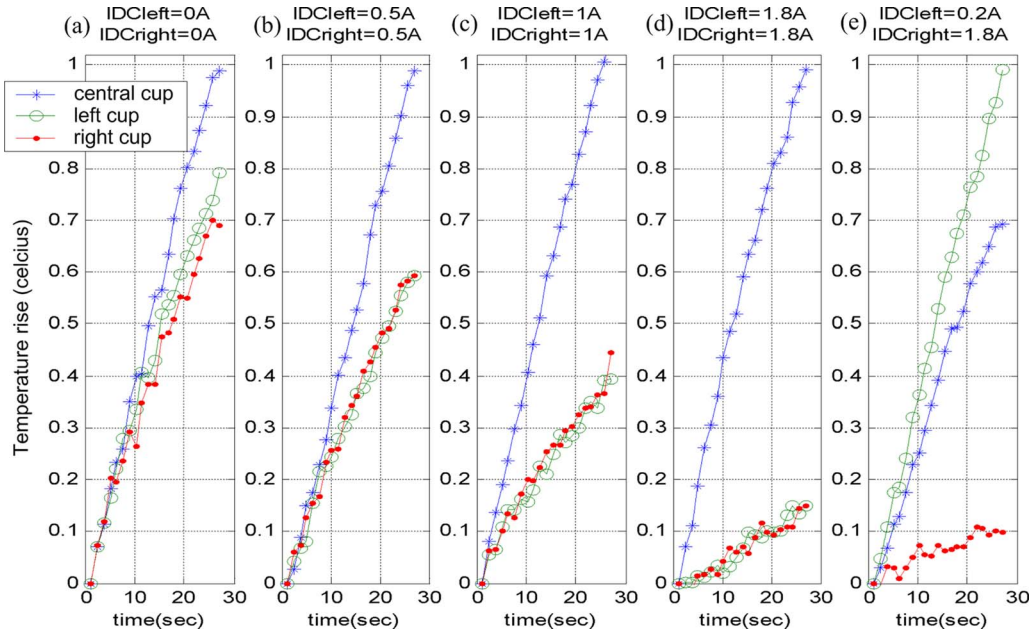

FIG. 3. Temperature rise versus time graphs of the *in vitro* experiments.

how the position of the field-free region shifts. Again, corresponding temperature rise data of the cups were obtained and analyzed in Sec. IV.

To visualize the dc magnetic field profile, and accordingly the SAR profile, magnetic field simulations were done by writing electromagnetic algorithms in MATLAB v7 (Mathworks, Inc., Natick, MA). The dc magnetic field profiles of the *in vitro* experiments were simulated and analyzed in Sec. IV.

III.B. *In vivo* experiments

In vivo experiments were performed on the tails of 200 g adult rats (obtained from Ankara Hospital Animal Experiment Laboratory). Magnetic fluids (Liquids Research Ltd., Bangor, Gwynedd, Wales, www.liquidsresearch.co.uk) used in the experiment consisted of superparamagnetic iron oxide particles (average core diameter: 10 nm) dispersed in water. The weight fraction of the iron was 20% and the saturation magnetization of the particles was 400 G. Magnetic fluids of 1.5 ml were injected percutaneously into the tails of the anesthetized rats and homogeneous distribution of the fluid was observed in the form of the tails' equally distributed color change. A tourniquet was made at the proximal end of the tails to prevent the diffusion of the magnetic fluid into the systemic blood circulation. After fluid injection, the rat tail was placed along the axis of the solenoids as shown in Fig. 2(b). A fiber optic temperature probe was placed in the tail portion, corresponding to the center of the FFR, to monitor the maximum temperature change in the tissue. Three rat experiments were performed where rats 1, 2, and 3 were exposed to static magnetic fields corresponding to 0.5, 1, and 1.8 A dc currents, respectively. In all experiments, an ac magnetic field with strength of 7.6 kA/m at 80 kHz was applied, and the resultant temperature increases were recorded. In addition to rats 1, 2, and 3, a control animal was used. Magnetic fluid was injected to the animal's tail but it was not treated with a magnetic field. In these *in vivo* experiments, the rat tail was used as a model because the tail constitutes the whole region in which the ac field exists. This helped us observe that some parts of the tail were not heated although they were exposed to the alternating magnetic field. In addition, since the tail is composed of different types of tissue such as bone, skin, and muscle, it is very suitable for detecting the effect of heating in different kinds of tissues.

For the histological examination, biopsy samples were obtained from the (a) region of interest (burned region), (b) its proximal parts, and (c) its distal parts. Those three tail parts are marked in the photographs shown in Fig. 5.

Those three regions (distal-burned-proximal) form the tail portion which resides inside the ac solenoid which is responsible for the heating of the particles. As a result, the total length of the distal-burned-proximal region was 6 cm which equals the length of the ac coil. The burned region was determined macroscopically where significant slimming and molting were observed on the rat tail (Fig. 5). The proximal and distal parts were 1.7–3 cm in length tail parts adjacent to the burned region. Tissue samples were retrieved, fixed in 10% phosphate buffered formalin (*p*H 7.0) at room temperature and rinsed in buffer. They were then decalcified in De Castro solution. Decalcified samples were washed under tap water, processed in graded series of ethanol, and embedded in paraffin. 5 μm thick serial sections were obtained with a sliding microtome (Leica, Germany) from each block stained with hematoxylin and eosin and Masson's trichrome. The former was used to evaluate the general morphology and the latter for the identification of connective tissue elements. Histological examination was performed by at least two independent investigators with a Leica DMR microscope (Germany). The images were captured via Leica DC500 digital camera (Germany).

TABLE I. Histological scoring system is presented. All specimens were graded according to these criteria.

		Score
Epidermis	Surface area of stratum spinosum affected by eosinophilic reaction (0%–100%)	0–4
	Stratum spinosum area filled with polymorphonuclear leukocytes (0%–100%)	0–4
	Stratum spinosum cystic areas (0%–100%)	0–4
	Area devoid of basal cells/basal cell involvement (0%–100%)	0–4
	Capillary vasocongestion of papillary layer (0%–100%)	0–3
Dermis	Reaction in connective tissue around capillaries:	
	✓ None	0
	✓ Fibroblastic	1
	✓ Fibroblastic+polymorphonuclear leukocytes or eosinophils	2
	✓ Fibroblastic+macrophages	3
	Changes in dermal collagen	
	✓ None	0
	✓ Granular collagen (papillary layer)	1
	✓ Loss of staining quality	2
	✓ Necrotic fiber	3
Maximum cumulative damage score		25

Histological observations were also graded in detail according to a histological skin damage scale (Table I).[13] All of the specimens were graded according to the histological scoring system shown in Table I. Cutaneous burns have been separated into three categories of severity: First-, second-, and third-degree burns.

IV. RESULTS

Temperature versus time graphs of the *in vitro* experiments are shown in Fig. 3. As can be seen in the figure, the temperature increase in the lateral cups (placed 2 cm away from the center) decreased as the amplitude of the dc solenoid currents (IDCleft and IDCright) increased. To the contrary, the temperature rise of the central cup was unaffected by the alteration of the dc field strength, as the cup was located in the field-free region.

Specific absorption rates of the cups were calculated as previously explained in Sec. III and the results are presented in Table II. The static magnetic fields that the cups experienced were also calculated and stated in Table II. To find the

TABLE II. SAR (W/kg) measurements of the magnetic fluid containing cups. The leftmost column shows the current magnitudes applied to solenoids. Subsequent columns show the static magnetic fields that each of the cups experienced and the resulting SAR values of the cups.

	The central cup		The lateral cup (left)		The lateral cup (right)	
dc solenoid current (A)	Static magnetic field (kA/m)	SAR (W/kg)	Static magnetic field (kA/m)	SAR (W/kg)	Static magnetic field (kA/m)	SAR (W/kg)
IDCleft=IDCright=0	0	160	0	120	0	110
IDCleft=IDCright=0.5	0	170	2.4	100	2.4	100
IDCleft=IDCright=1.0	0	170	4.8	60	4.8	60
IDCleft=IDCright=1.8	0	160	8.6	30	8.6	30
IDCleft=0.2 IDCright=1.8	2.9	120	0.2	160	9.8	20

magnetic field generated by the solenoids, we first calculated the magnetic field produced by a single current loop and then superimposed this solution for the current loops of the solenoids.

As we can see from Table II, while the current of the dc solenoids increased from 0 to 1.8 A, the SAR of the lateral cups decreased from 120 to 30 W/kg and the SAR of the central cup did not change, remaining at roughly 160 W/kg.

Another *in vitro* experiment was done to observe the shifting of the FFR through the application of different magnitudes of currents (IDC) to the dc solenoids. In this case, 0.2 A was applied to the solenoid on the left-hand side and 1.8 A was applied to the solenoid on the right-hand side. The corresponding temperature curve is shown in Fig. 3(e). Looking at this figure, one can observe that maximum heating was seen in the left cup, demonstrating that the field-free region shifted to the left.

To visualize the dc magnetic field strength generated by the dc solenoids, we made electromagnetic simulations as explained in Sec. III. Figure 4(a) shows the dc magnetic field profiles corresponding to dc solenoid currents of 0.5, 1, 1.8, and 20 A. As shown in the figure, as we increased the current from 0.5 to 1.8 A, the dc magnetic field gradient at the center increased and the dc field started to dominate the ac magnetic field (4500 A/m). As a result, we got more intense focus at the center. To visualize the magnetic field profile corresponding to higher currents, we made a simulation for a solenoid current of 20 A. As can be seen in Fig. 4(a), for such a high current we obtained a very sharp dc field gradient at the center and the dc field started to dominate the ac field (4500 A/m) at the very vicinity of the center so that we could get a very intense heating focus at the center of the system.

In Fig. 4(b), the shifting of the heating focus is simulated for solenoid currents of IDCleft=0.2 A and IDCright =1.8 A, and the FFR is shifted approximately 2 cm to the left. This verifies that heating is focused on the left magnetic fluid cup, which was placed 2 cm to the left of the center.

By looking at Fig. 4(b), one can observe that the shape of the magnetic field for IDCleft=0.2 A and IDCright=1.8 A differs from the shape of the magnetic field for IDCleft =1.8 A and IDCright=1.8 A, such that the intensity of the focus decreased (FFR broadened). This also verifies the experimental results of Fig. 3(e). As shown in Fig. 3(e), we have the maximum temperature increase in the left cup but also we have a significant temperature rise in the central cup. This is because of the broadening of the FFR. If we want to preserve the shape of the FFR, we should apply currents of IDCleft=0.6 A and IDCright=5.4 A, as shown in Fig. 4(b).

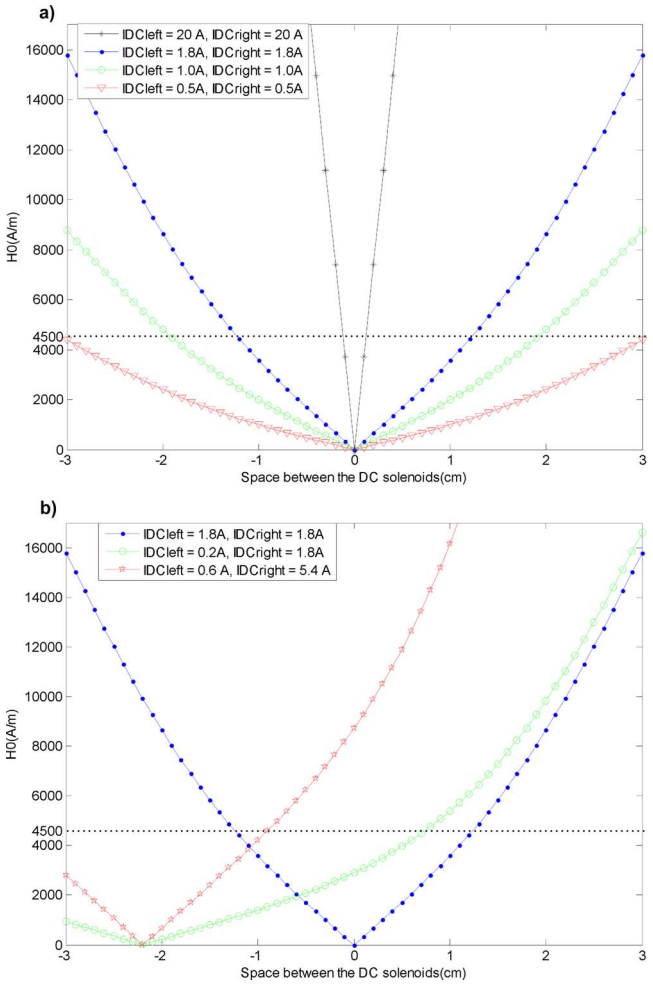

FIG. 4. Simulation of the dc magnetic field strength (H0) between the dc solenoids. 4500 A/m is shown with a dashed line which was the ac magnetic field applied between the dc solenoids. (a) For the solenoid currents of IDCleft=IDCright=0.5, 1, 1.8, and 20 A. (b) For the solenoid currents of IDCleft=1.8 A, IDCright=1.8 A; IDCleft=0.2 A, IDCright=1.8 A; and IDCleft=0.6 A, IDCright=5.4 A.

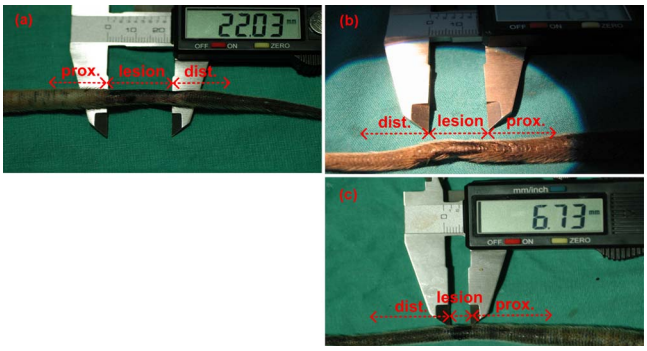

FIG. 5. Rat tail photographs 24 h after the hyperthermia application. Burned regions are marked and measured by a vernier caliper. For the histological examination, samples were taken from the lesion, proximal, and distal parts. (a) Rat 1 (IDC=0.5 A, lesion≈2.2 cm). (b) Rat 2 (IDC=1 A, lesion ≈1.5 cm). (c) Rat 3 (IDC=1.8 A, lesion≈0.7 cm).

As explained in Sec. III, *in vivo* hyperthermia experiments were performed for three different dc field strengths on rats 1–3. ac field exposure lasted nearly 25 min and temperatures above 46 °C were obtained at the center of the FFR for all three experiments. 24 h after the experiments, significant slimming and molting were observed on all three of the rat tails. As shown in the photographs of Fig. 5, the size of the lesion (burned region) decreased as the applied static magnetic field strength increased.

The width of the lesion regions of the tails were measured with a caliper and the sizes of about 2.2, 1.5, and 0.7 cm were obtained in rats 1, 2, and 3, corresponding to dc solenoid currents of 0.5, 1, and 1.8 A, respectively. Tail photographs macroscopically confirmed that hyperthermia with higher focus was achieved as the currents of the dc solenoids were increased.

Histological scores of damage are presented with the bar graph shown in Fig. 6. Damage was not observed at the proximal and distal parts of the lesion region. Rat tails of the proximal and distal were relatively intact. Some of the specimens exhibited minor changes, including capillary congestion and edema. On the other hand, cellular infiltration was obvious in all the specimens. The lesion (burned region) was generally characterized by a second-degree burn varying in size between rats 1–3. Desquamated epidermis, dermal cysts, granular appearance of dermal collagen, and vascular congestion were present in these specimens. In some of the sections, a third-degree burn was noted. Necrotic dermal collagen fibers and disrupted bone and cartilage matrices were present on these specimens.

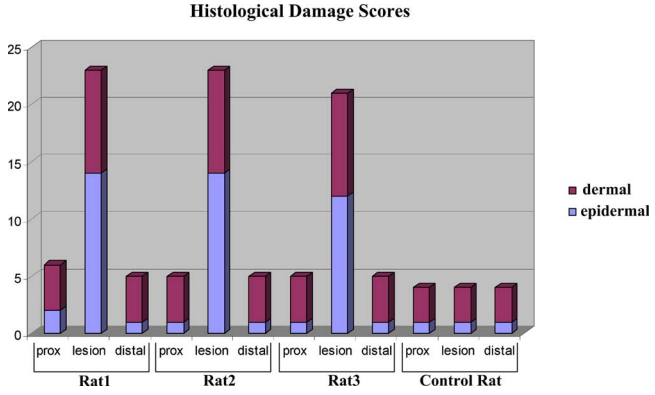

FIG. 6. Histological scores of damage for the rat tails' proximal (prox), distal, and lesion-containing portions.

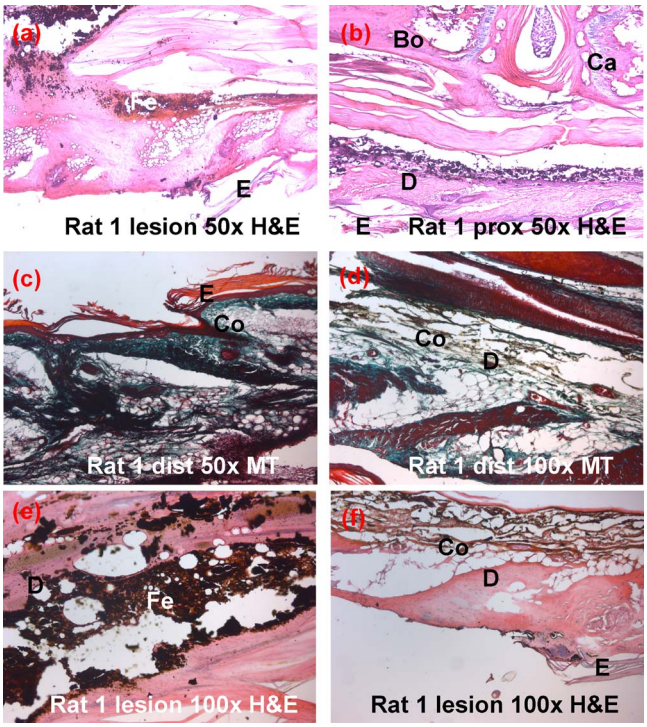

FIG. 7. (Rat 1) Second-degree burn is observed in (a) characterized by the lost of epidermis (e). Proximal (prox) and distal (dist) portions appear normal with the healthy distribution of dermal (d), connective tissue elements including collagen (Co) fibers, cartilage (Ca), and bone (Bo) cellular elements. Ferrofluid particles invaded the dermis. They are surrounded by phagocytic cells in (e). Granular collagen is present in dermis (d) at lesion site of rat 1 in (f). H&E: Hematoxylin & eosin, MT: Masson's trichrome.

Sample histological pictures of the specimens taken from the lesion, proximal, and distal parts of the tail of rat 1 can be seen in Fig. 7. The second- and third-degree burned regions were observed at the lesion side of the tails. The total burned volume of rats 1–3 was calculated by summing up the sizes of the second- and third-degree burn areas; results are stated in Table III.

V. DISCUSSION

In this study, we have shown that focused heating of magnetic domains can be achieved successfully by depositing dc field gradients on ac fields such that a region free of dc magnetic field (FFR) is produced in the presence of ac mag-

TABLE III. Total second-/third-degree burn volumes observed in the rat tails.

	Rat 1 (IDC=0.5 A)	Rat 2 (IDC=1 A)	Rat 3 (IDC=1.8 A)
Burned volume (cm^3)	1.56	0.29	0.17

netic field. As demonstrated in the temperature versus time graphs of Fig. 3 and SAR measurements of Table II, the intensity of the heating focus can be easily improved by increasing the dc magnetic field gradient, i.e., by applying higher magnitudes of currents to the dc solenoids.

As shown in the magnetic field simulations [Fig. 4(a)], if we want to focus the heat at the center of the solenoids, both solenoids should be excited with the same dc currents. If we want to change the position of the focus (FFR), we should apply different amounts of currents to the solenoids but, to preserve the intensity of the focus, these currents should be selected carefully by making magnetic field simulations as shown in Fig. 4(b).

Heat focusing ability of the hyperthermia system was verified *in vivo* via rat experiments. As summarized in Table III, we obtained a significant decrease in the total burned volume as we increased the magnitude of the static magnetic field.

The system implemented in this study can shift the focus in only one dimension (along the axis of the solenoids). 3D movement of the focus could be achieved by using more dc coils which could shift the FFR along the x, y, and z axes. For this purpose, 3D gradient coil systems similar in shape to the gradient coils of magnetic resonance imaging (MRI) scanners may be used. Typical MRI gradient coils produce dc field gradients in all three dimensions. Through further optimization of this gradient coil system, 3D scanning of the heat focus could be obtained. Using such 3D location-shifting approach, tumors with different geometries can be treated by moving the FFR over the tumor. Even with the presented hyperthermia system (composed of two dc solenoids), tumors with various shapes might still be treated. To achieve this, since the FFR region always stays at the center, the patient would have to be moved by very accurate robotic devices according to the shape of the tumor.

Copper heating is one of the serious problems that should be considered during the design of the magnetic field applicators. In our system copper heating was seen in both dc and ac field applicators and heating was resolved by using water cooling. Water cooling setups are successful in preventing the copper heating of ac field applicators with magnetic field amplitudes lower than 20 kA/m.[14] Water cooling may not be sufficient for dc field applicators if highly intense focus is needed (i.e., very large magnitudes of dc current flow is necessary). To address this problem, superconductive wires could be utilized in the construction of the dc field applicators.

VI. CONCLUSION

A novel hyperthermia system, capable of focused heating of tumors, is presented and verified through experiments. Through the use of this newly developed heat treatment system, magnetic fluid hyperthermia can be a more effective heat treatment method, with a much decreased risk of heating healthy collateral tissues. Future works can include the combination of the hyperthermia system with a suitable imaging method and the construction of the dc solenoids with superconductive wires to overcome the excessive copper heating. In addition, systems capable of 3D shifting of the heating focus can also be implemented. Furthermore, primary concern should be given to the optimization of the magnetic fluids, which will lead to the heating of tumors with very small amounts of fluid injections and very short treatment durations.

ACKNOWLEDGMENTS

This work has been supported by a grant from the National Institutes of Health (Grant No. R01-RR-15396) and European Commission, FP6 Marie Curie International Reintegration Grant.

[a]Author to whom correspondence should be addressed. Electronic mail: ergin@ee.bilkent.edu.tr

[1]P. Moroz, S. K. Jones, and B. N. Gray, "Magnetically mediated hyperthermia: Current status and future directions," Int. J. Hyperthermia **18**, 267–284 (2002).
[2]P. Moroz, S. K. Jones, and B. N. Gray, "Status of hyperthermia in the treatment of advanced liver cancer," J. Surg. Oncol. **77**, 259–269 (2001).
[3]M. Shinkai, "Functional magnetic particles for medical application," J. Biosci. Bioeng. **94**, 606–613 (2002).
[4]M. Johannsen, A. Jordan, R. Scholz, M. Koch, M. Lein, S. Deger, J. Roigas, K. Jung, and S. Loening, "Evaluation of magnetic fluid hyperthermia in a standard rat model of prostate cancer," J. Endourol. **18**, 495–500 (2004).
[5]A. Jordan, P. Wust, H. Fahling, W. John, A. Hinz, and R. Felix, "Inductive heating of ferrimagnetic particles and magnetic fluids: Physical evaluation of their potential for hyperthermia," Int. J. Hyperthermia **9**, 51–68 (1993).
[6]F. Matsuoka, M. Shinkai, H. Honda, T. Kubo, T. Sugita, and T. Kobayashi, "Hyperthermia using magnetite cationic liposomes for hamster osteosarcoma," BioMagnetic Research and Technology 2004, 2:3.
[7]B. Gleich and J. Weizenecker, "Tomographic imaging using the nonlinear response of magnetic particles," Nat. Biotechnol. **435**, 1214–1217 (2005).
[8]W. F. Brown, Jr., "Thermal fluctuations of a single-domain particle," Phys. Rev. **130**, 1677–1686 (1963).
[9]L. Neel, "Theorie du trainage magnetique des ferromagnetiques en grains fins avec applications aux terres cuites," Ann. Geophys. **5**, 99–136 (1949).
[10]M. Babincova, D. Leszczynska, P. Sourivong, P. Cicmanec, and P. Babinec, "Superparamagnetic gel as a novel material for electromagnetically induced hyperthermia," J. Magn. Magn. Mater. **225**, 109–112 (2001).
[11]B. B. Austin, "The effective resistance of inductance coils at radio frequency," *The Wireless Engineer*, Vol. 11, pp. 12–16, Jan. 1934, summary of work by S. Butterworth.
[12]P. N. Murgatroyd, "Calculation of proximity losses in multistranded conductor bunches," Proc. IEEE **36**, 115–120 (1989).
[13]P. F. Meyer, P. D. Gadsby, D. Van Sickle, W. E. Schoenlein, K. S. Foster, and G. P. Graber, "Impedance-gradient electrode reduces skin irritation induced by transthoracic defibrillation," Med. Biol. Eng. Comput. **43**, 225–229 (2005).
[14]S. Mornet, S. Vasseur, F. Grasset, and E. Duguet, "Magnetic nanoparticle design for medical diagnosis and therapy," J. Mater. Chem. **14**, 2161–2175 (2004).